MAGNETIC RECONNECTION

MHD Theory and Applications

ERIC PRIEST
Department of Mathematical and Computational Sciences
University of St. Andrews

TERRY FORBES
Institute for the Study of Earth, Oceans, and Space
University of New Hampshire

CAMBRIDGE
UNIVERSITY PRESS

PUBLISHED BY THE PRESS SYNDICATE OF THE UNIVERSITY OF CAMBRIDGE
The Pitt Building, Trumpington Street, Cambridge, United Kingdom

CAMBRIDGE UNIVERSITY PRESS
The Edinburgh Building, Cambridge CB2 2RU, UK http://www.cup.cam.ac.uk
40 West 20th Street, New York, NY 10011-4211, USA http://www.cup.org
10 Stamford Road, Oakleigh, Melbourne 3166, Australia
Ruiz de Alarcón 13, 28014 Madrid, Spain

First published 2000

Printed in the United States of America

Typeface in Computer Modern 10/12.5 pt. *System* LaTeX [TB]

A catalog record for this book is available from
the British Library.

Library of Congress Cataloging in Publication Data
Priest, E. R. (Eric Ronald), 1943–
Magnetic reconnection : MHD theory and applications / Eric Priest,
Terry Forbes.
p. cm.
ISBN 0-521-48179-1
1. Magnetic reconnection. 2. Space plasmas. 3. Plasma (Ionized gases)
4. Magnetohydrodynamics
I. Priest, Eric R. 1943– , II. Forbes, Terry, G. 1946– . III. Title.
QC809.P5P75 1999
523.01′886 – dc21 99-14939
CIP

ISBN 0 521 48179 1 hardback

Contents

1
Introduction

Like most fundamental concepts in physics, magnetic reconnection owes its appeal to its ability to unify a wide range of phenomena within a single universal principle. Virtually all plasmas, whether in the laboratory, the solar system, or the most distant reaches of the universe, generate magnetic fields. The existence of these fields in the presence of plasma flows inevitably leads to the process of magnetic reconnection. As we shall discuss in more detail later on, reconnection is essentially a topological restructuring of a magnetic field caused by a change in the connectivity of its field lines. This change allows the release of stored magnetic energy, which in many situations is the dominant source of free energy in a plasma. Of course, many other processes besides reconnection occur in plasmas, but reconnection is probably the most important one for explaining large-scale, dynamic releases of magnetic energy.

Figures 1.1–1.4 illustrate the rich variety of plasma environments where reconnection occurs or is thought to occur. The evidence of reconnection in laboratory fusion machines such as the tokamak [Fig. 1.1(a)] and the reversed-field pinch [Fig. 1.1(c)] is so strong that there is no longer any controversy about whether reconnection occurs, but only controversy about the way in which it occurs (§9.1). However, as one considers environments which are further away from the Earth, the evidence for reconnection becomes more circumstantial. Most researchers who study the terrestrial aurorae [Fig. 1.2(a)] believe that they are directly or indirectly the result of reconnection in the Earth's magnetosphere, but the evidence for similar phenomena in other planetary magnetospheres [Fig. 1.2(b)] is much smaller (§10.6). It has also been argued that reconnection lies at the root of phenomena called disconnection events which occur in comet tails [Fig. 1.2(c)].

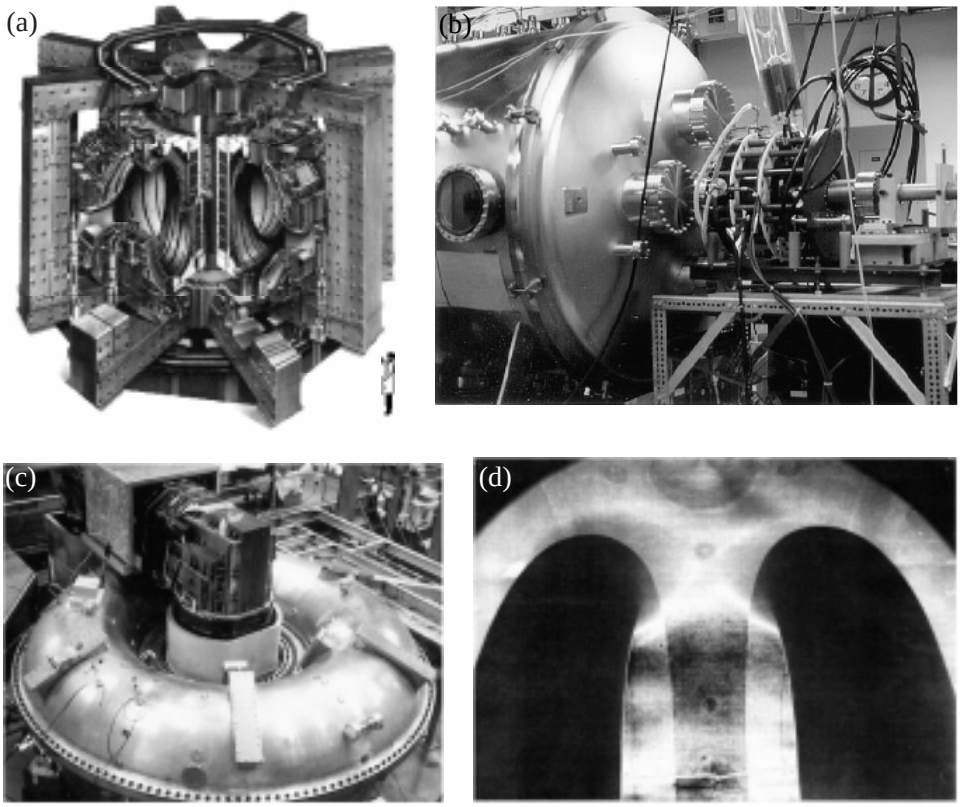

Fig. 1.1. Laboratory Plasmas. (a) Drawing of the Joint European Torus (JET) located in England. The scale is given by the figure at lower right (courtesy of JET Joint Undertaking). (b) Plasma injection gun of the Swarthmore Spheromak (courtesy of M.R. Brown). (c) Reversed-field-pinch device at the University of Wisconsin (courtesy of R. Dexter, S. Prager, and C. Sprott). (d) Interior photograph of the MRX reconnection experiment at the Princeton Plasma Physics Laboratory taken during operation. In the region at the top, between the two dark toroidal coils, a magnetic X-line is outlined by a bright emission, which comes primarily from the Hα Balmer line of hydrogen (courtesy of M. Yamada).

Even though the Sun is a rather distant object compared with the aurora, some of the best evidence for reconnection is to be found there. Reconnection provides an elegant, and so far the only, explanation for the motion of chromospheric ribbons and flare loops during solar flares [Fig. 1.3(b)]. At the same time, it also accounts for the enormous energy release in solar flares. The ejection of magnetic flux from the Sun during coronal mass ejections and prominence eruptions [Fig. 1.3(a)] necessarily requires reconnection; otherwise, the magnetic flux in interplanetary space would build up indefinitely (§11.4.1). Reconnection has also been proposed as a

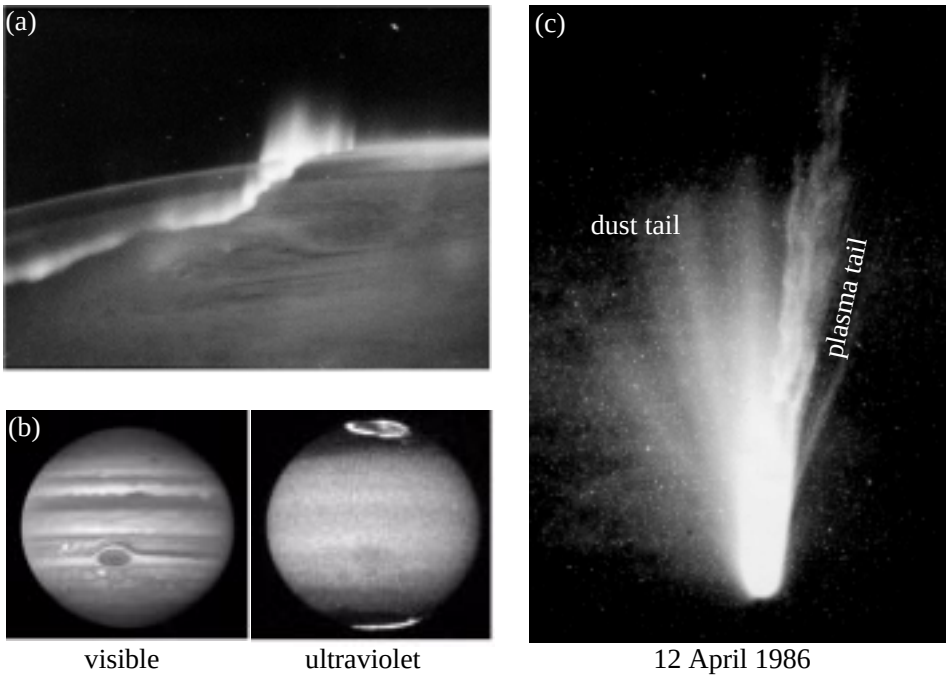

Fig. 1.2. Planets and Comets. (a) Aurora Australis photographed over Antarctica by the space shuttle Discovery (NASA). (b) The Jovian aurora as observed by the Wide-Field Planetary Camera 2 on the Hubble Space Telescope. Auroral ovals are visible at both poles in the ultraviolet image, which was taken 15 min after the visible image (courtesy of John T. Clarke). (c) Disconnection of the plasma tail of comet Halley during its 1986 appearance. The image is a 3-min exposure taken by the Michigan Schmidt Telescope at the Cerro Tololo Inter-American Observatory (produced by Jet Propulsion Laboratory/NASA).

mechanism for the heating of solar and stellar coronae to extremely high temperatures [$>10^6$ K; Fig. 1.3(c)]. Even more fundamental is the role played by reconnection in the generation of solar, stellar, and planetary magnetic fields. The generation of magnetic fields in astrophysics and space physics is based almost exclusively on the concept of a self-excited magnetic dynamo. In a dynamo, complex motions of a plasma with a weak seed magnetic field can generate a stronger large-scale magnetic field. Magnetic reconnection is an essential part of this generation process, so, in this sense, the very existence of all magnetic phenomena on the Sun such as prominences, flares, the corona, and sunspots (Fig. 1.3) requires reconnection (Cowling, 1965).

The role of reconnection in plasma environments beyond the solar system remains both speculative and controversial. Because of the great distances involved, observations provide very few facts with which to constrain

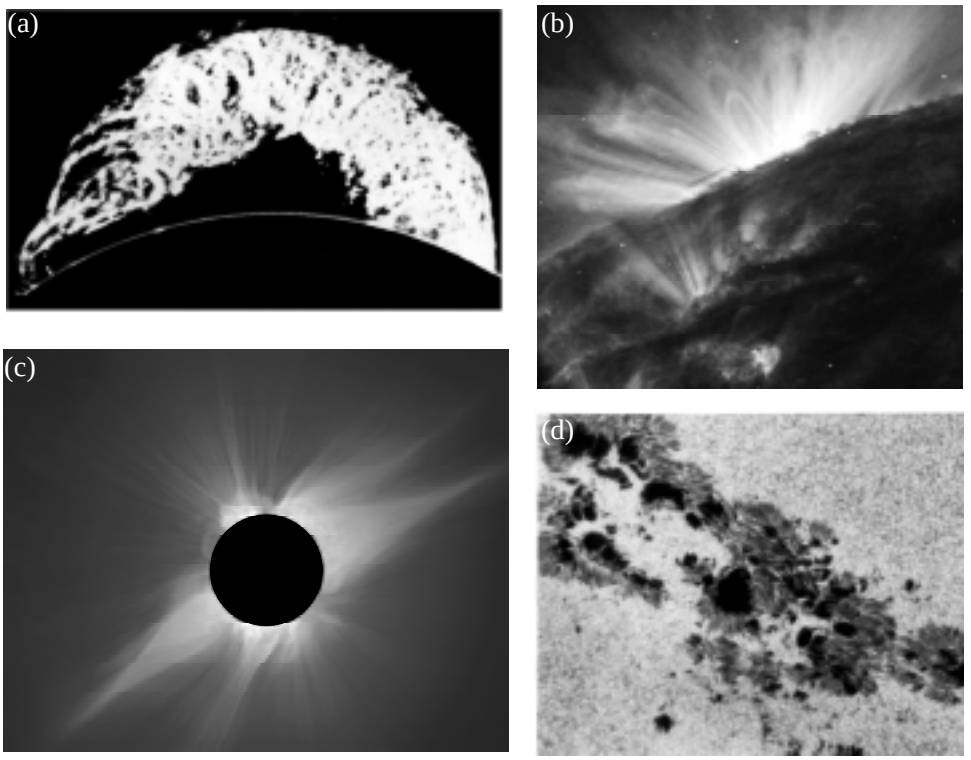

Fig. 1.3. The Sun. (a) Hα photograph of the extremely large prominence eruption (known as "Grandaddy") which occurred on 4 June 1946 (courtesy of the High Altitude Observatory). (b) X-ray image of the west limb of the Sun in Fe IX/X lines obtained by TRACE (Transition Region and Coronal Explorer) on 24 April 1998. On the limb is a system of "post"-flare loops, while in the centre foreground is an X-ray bright "point." Both features are thought to be produced by reconnection (courtesy of A. Title and L. Golub). (c) Solar corona photographed from Baja California, Mexico during the total eclipse on 11 July 1991 (courtesy of S. Albers). (d) Sunspots (courtesy of the National Solar Observatory at Sacramento Peak, New Mexico).

theories. One of the main reasons that reconnection is often invoked in astrophysical phenomena such as stellar flares [Fig. 1.4(a)] or galactic magnetotails is that these phenomena may be analogues of the same processes occurring in the solar corona and the Earth's magnetosphere. However, reconnection has also been invoked to account for viscous dissipation in accretion disks [Fig. 1.4(b)], for which no counterpart exists in the solar system. It may even be involved in the formation of chondritic inclusions in certain types of meteorite [Fig. 1.4(c)]. The most popular theory for the formation of these inclusions is that they were formed by reconnection in the

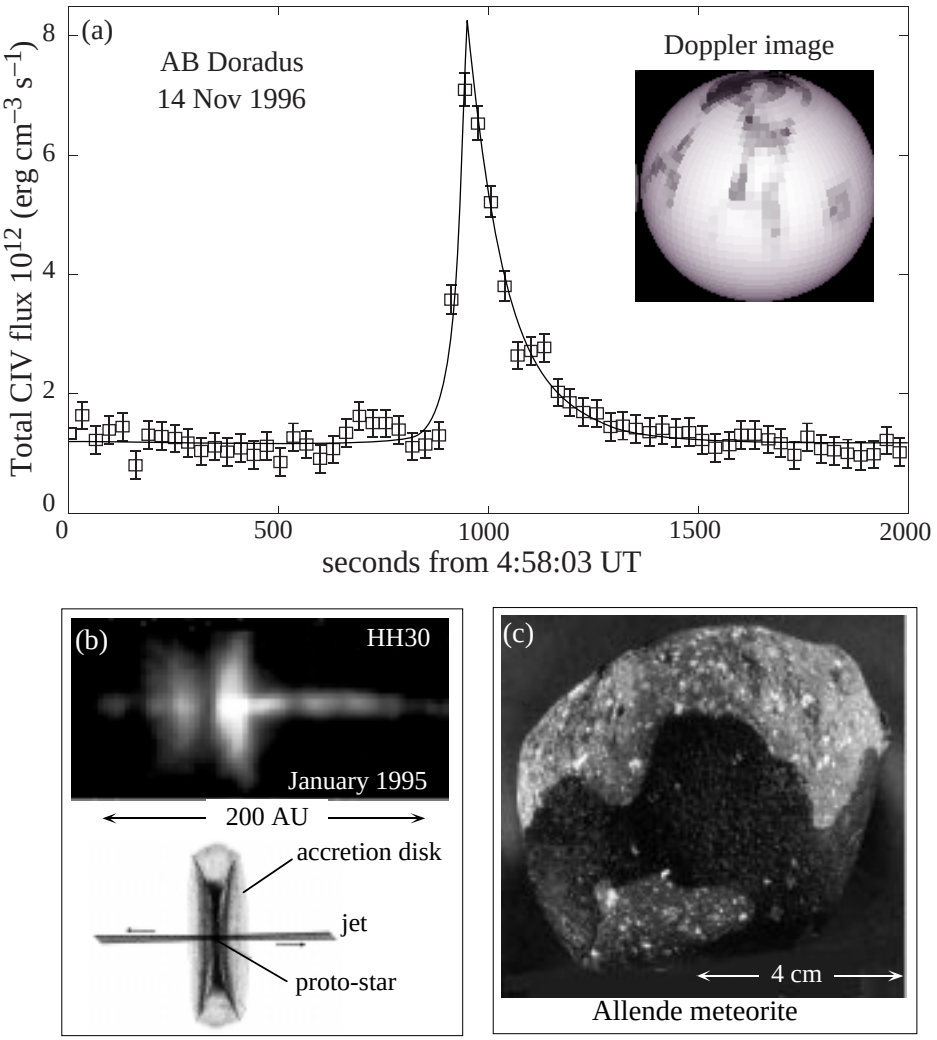

Fig. 1.4. Astrophysics. (a) Light-curve in the UV carbon IV line obtained by the Hubble Space Telescope of an impulsive flare on AB Doradus (Vilhu et al., 1998). The inset shows a Doppler image of AB Doradus constructed from photospheric spectral lines over a period of several hours on a different date. The dark areas are strongly magnetized regions which are the stellar equivalent of sunspots (courtesy of A.C. Cameron). (b) Hubble Space Telescope image of the accretion disk around the protostellar object called HH-30, which is 450 light years away in the constellation Taurus. The disk is seen edge on, and the light from the forming star illuminates both the top and bottom surfaces of the disk. The star itself is hidden behind the densest parts of the disk (courtesy of C. Burrows). (c) Part of the Allende meteorite, which struck the region of Chihuahua, Mexico, on 8 February 1969. It contains chondritic inclusions that are thought to have been created by nebular flares in the accretion disk which surrounded the Sun during its formation (courtesy of E.A. King).

accretion disk which existed during the early phase of the formation of the solar system. According to this theory, the reconnection of magnetic fields in the dust-filled disk produced solar nebular flares, which welded the dust into the inclusions found in many carbonaceous meteorites.

The occurrence of magnetic reconnection in a wide variety of plasma environments makes it a topic in which researchers from many different disciplines contribute to the understanding of a fundamental plasma process. From a theoretical perspective, reconnection is especially challenging because it involves nonlinear, non-ideal processes in an inherently complex magnetic topology.

1.1 The Origins of Reconnection Theory

Interest in magnetic reconnection has continually grown since it was first proposed in the 1940s. The reasons for this growth are varied, but the most important is the realisation that reconnection is necessary for the efficient release of energy stored in planetary, solar, stellar, and astrophysical magnetic fields.

In MHD theory, processes which convert magnetic energy into other forms can be distinguished as ideal or non-ideal. Ideal processes, such as the ideal kink instability, convert magnetic energy into kinetic energy without magnetic dissipation, while non-ideal processes, such as magnetic reconnection, can convert magnetic energy into kinetic energy and heat. Because they lack dissipation, ideal processes cannot generate heat (i.e., raise the entropy). Yet, in practice, they typically generate compressive waves which steepen nonlinearly to form shock waves no matter how small the dissipation is. The dissipation in such shocks is thus an important non-ideal process which converts motions of an ideal process into heat.

In space physics the distinction between ideal and non-ideal processes is important because simple estimates imply that magnetic dissipation acts on a time-scale which is many orders of magnitude slower than the observed time-scales of dynamic phenomena. For example, solar flares release stored magnetic energy in the corona within a period of 100 s. By comparison, the time-scale for magnetic dissipation based on a global scale-length of 10^5 km is of the order of 10^6 yr. Typically, phenomena like the solar flare and the substorm require a significant fraction of the stored magnetic energy to be converted within a few Alfvén time-scales. Such rapid time-scales are easily achieved in ideal MHD processes but not in non-ideal ones. Although ideal MHD processes can release energy quickly, they rarely release a significant amount because of the topological constraints which exist in the absence

of dissipation. In contrast, magnetic reconnection is not topologically constrained, and therefore it can release a much greater amount of magnetic energy (Kivelson and Russell, 1995).

One of the principal goals of reconnection theory is to explain how reconnection can occur on short enough time-scales (although very recently there has been a shift in emphasis to explore the three-dimensional aspects, as described in Chapter 8). Historically, two approaches have been adopted. The first, based on the kinetic theory of plasmas, has been to find an anomalous resistivity mechanism which will allow rapid dissipation. The second approach, based on MHD (the main focus of this book), has been to find a geometrical configuration which greatly reduces the effective dissipation scale-length. These two approaches are often combined in analyzing specific phenomena.

For example, the ion-tearing mode, which is a wave-particle theory of reconnection, has been proposed as a mechanism for the onset of reconnection in the geomagnetic tail at the start of an auroral substorm (§10.5). However, in order for the ion-tearing mode to occur, it is first necessary that the current sheet in the tail become very much thinner than normal. Usually, the width of the current sheet is of the order of 7000 km (approximately an Earth radius), but the ion-tearing mode becomes effective only when the width is of the order of 200 km (approximately an ion-gyro radius). Recent observations that such thinning of the current sheet actually occurs at substorm onset has motivated researchers to develop MHD models to explain how conditions in the solar wind upstream of the Earth initiate the thinning in the tail (§10.5).

The process of magnetic reconnection has its origins in suggestions by R.G. Giovanelli (1946) and F. Hoyle (1949) that magnetic X-type null points can serve as locations for plasma heating and acceleration in solar flares and auroral substorms. Their interest in X-points may have been due to the fact that a magnetic field tends to inhibit particle acceleration unless the electric field has a component parallel to the magnetic field. Early researchers usually assumed that electrons quickly short out any parallel electric field, so magnetic null regions (or points) were thought to offer the best locations for particle acceleration. Magnetic null points occur naturally when there are two or more sources of magnetic field, such as the Sun and the Earth, for example. If an electric field exists in the vicinity of such a null point, then charged particles there will undergo acceleration until they travel into a region where the magnetic field is no longer negligible. This view of acceleration is now somewhat outdated, because many mechanisms have since been proposed for particle acceleration which do not require a null point (see Lyons and

Williams, 1984, or Tandberg-Hanssen and Emslie, 1988, for example). These mechanisms use electric and magnetic fields which are nonuniform in space and sometimes in time (see Chapter 13).

Cowling (1953) pointed out that, if a solar flare is due to ohmic dissipation, a current sheet only a few metres thick is needed to power it. Then J.W. Dungey (1953), who was a student of Hoyle, showed that such a current sheet can indeed form by the collapse of the magnetic field near an X-type neutral point, and he was the first to suggest that "lines of force can be broken and rejoined." He considered the self-consistent behaviour of both field and particles at an X-point (see §1.3.1). This is a quite different approach from simply considering the motion of charged particles in a given set of electric and magnetic fields. Moving charged particles are themselves a source of electric and magnetic fields, and in a plasma these self-fields must be taken into account by combining Maxwell's equations with Newton's equations of motion. To analyze the effect of such fields, Dungey used the MHD equations for a plasma with negligible gas pressure, and he found that small perturbations in the vicinity of the null point lead to the explosive formation of a current sheet (§2.1). Near the null point, plasma motions induced by a small current perturbation cause the current to grow, and this current further enhances the plasma motions resulting in a positive feedback.

After Dungey's pioneering work on the formation of current sheets, P.A. Sweet (1958a,b) and E.N. Parker (1957) were the first to develop a simple MHD model for how steady-state reconnection might work in a current sheet formed at a null point (§4.2). At the 1956 symposium in Stockholm, Sweet (1958a) stressed that conditions far from an X-point, as well as plasma pressure, may play important roles in forming a current sheet. As a model for solar flares, he considered a magnetic field with an X-point produced by sources in the photosphere. If the sources approach one another and the magnetic field remains frozen to the plasma, a narrow "colliding layer" (Sweet's term) forms around the null point. The field flattens, and magnetohydrostatic equilibrium implies that the plasma pressure inside the layer, or current sheet, is the same as the external magnetic pressure. Plasma is squeezed out of the ends of the sheet by this excess pressure, just as a fluid would be squeezed out between approaching plates. Parker, while listening to Sweet's talk, realised how to model the process in terms of MHD and so eagerly went back to his room on the evening of Sweet's talk and worked out the details. Parker derived scaling laws for the process and coined the words "reconnection of field lines" and "merging of magnetic fields" (Parker, 1957). Later Parker (1963) also coined the phrase "annihilation of magnetic fields" and gave an in-depth development of the mechanism. He modelled the internal structure

across the current sheet and, in passing, made the challenging comment that "it would be instructive if the exact equations could be integrated on a machine," a challenge that took nearly thirty years to be accomplished reasonably and which still needs a full treatment. In the same paper, he also included compressibility and other effects for enhancing reconnection, such as ambipolar diffusion and fluid instabilities. He then applied this quantitative model to solar flares, but he found that the rate at which magnetic energy is converted to kinetic energy and heat is far too slow (by a factor of at least a hundred) to account for flares. A conversion rate several orders of magnitude greater was needed to explain the energy release in solar flares, and thus the Sweet–Parker model is often referred to as a model for *slow* reconnection. Ever since Sweet and Parker presented their model, the search has continued for a reconnection process which would be fast enough to work for solar flares.

As we mentioned previously, there have been two separate approaches in the search for a theory of fast reconnection – one based on showing that the plasma resistivity is sufficiently high, the other based on showing that the dissipation scale is sufficiently small. In calculating the reconnection rate, Sweet and Parker assumed that Spitzer's (1962) formula for the resistivity can be applied to the corona. However, there is good reason to suspect that Spitzer's formula is not valid for the type of plasma that is produced in the corona during a flare, since it assumes that there are many more collisions between particles than is appropriate for the solar corona or many other space and astrophysical plasmas. Thus, Sweet and Parker's mechanism might be fast enough only when combined with an anomalous resistivity.

The length of the current sheet in Sweet and Parker's model is approximately the same as the global scale-length of the flaring region. However, Petschek (1964) developed an alternative model with a current sheet whose length is many orders of magnitude smaller than the one assumed by Sweet and Parker (§4.3). Because of this much smaller current sheet, Petschek's model predicts a reconnection rate which is close to the rate needed in solar flares, even if Spitzer resistivity is assumed. Thus, Petschek's model was the first model of *fast* reconnection to be proposed. Since then, a new generation of more general almost-uniform (§5.1) and non-uniform (§5.2) models has been developed.

One of the most important developments in the theory of reconnection occurred at about the same time when Furth, Killeen, and Rosenbluth published their classic paper on the tearing mode (Furth et al., 1963). In this paper they analyzed the stability of a simple, static current sheet and found that a sheet whose length is at least 2π times greater than its width will

spontaneously reconnect to form magnetic islands (see Chapter 6). Thus, although in some applications reconnection occurs as a steady or quasi-steady process (i.e., modulated on a time-scale longer than the reconnection time), in other applications the reconnection is inherently time-dependent with impulsive and bursty releases of energy.

1.2 Magnetohydrodynamic Equations

Since derivations of the magnetohydrodynamic (MHD) equations are readily available elsewhere (e.g., Roberts, 1967; Priest, 1982), we give here only a short summary of them. The limitations of the MHD equations, especially regarding their use in collisionless plasmas, are discussed briefly in Section 1.7. MKS units are adopted, but their relationship to cgs units is summarised in Appendix 2, so that, for example, magnetic fields are measured in tesla, where 1 tesla $= 10^4$ gauss. The shorthand (G) for gauss is used, but the usual shorthand (T) for tesla is not used here in order to avoid possible confusion with the symbol (T) for temperature.

1.2.1 Basic Equations

The MHD equations embody the following conservation principles derived from the equations of fluid mechanics and electromagnetism.

Mass conservation:

$$\frac{d\rho}{dt} \equiv \frac{\partial \rho}{\partial t} + \mathbf{v} \cdot \nabla \rho = -\rho \nabla \cdot \mathbf{v}, \tag{1.1}$$

where ρ is the mass density, $\mathbf{v}$ is the bulk flow velocity, t is the time, and d/dt is the convective derivative, which represents the time rate of change following a plasma element as it moves.

Momentum conservation:

$$\rho \frac{d\mathbf{v}}{dt} = -\nabla p + \mathbf{j} \times \mathbf{B} + \nabla \cdot \underline{\mathbf{S}} + \mathbf{F}_g, \tag{1.2}$$

where p is the plasma pressure, $\mathbf{j}$ is the current density, $\mathbf{B}$ is the magnetic induction, $\underline{\mathbf{S}}$ is the viscous stress tensor, and $\mathbf{F}_g$ is an external force such as gravity. The induction ($\mathbf{B}$) is usually referred to as the "magnetic field," although technically the magnetic field is $\mathbf{H} = \mathbf{B}/\mu$, where μ is the magnetic permeability of free space ($4\pi \times 10^{-7}\,\mathrm{H\,m^{-1}}$).

In very weak magnetic fields the stress-tensor components are

$$S_{ij} = \rho\left(\zeta - \frac{2\nu}{3}\right)\nabla \cdot \mathbf{v}\,\delta_{ij} + \rho\nu\left(\frac{\partial v_i}{\partial x_j} + \frac{\partial v_j}{\partial x_i}\right), \tag{1.3}$$

where ν and ζ are the coefficients of kinematic shear and bulk viscosity, respectively. The divergence of this expression (when the dynamic viscosity $\rho\nu$ and bulk viscosity $\rho\zeta$ are assumed uniform) gives the viscous force

$$\nabla \cdot \underline{\mathbf{S}} = \rho\nu\nabla^2\mathbf{v} + \rho(\zeta + \nu/3)\nabla(\nabla \cdot \mathbf{v}). \tag{1.4}$$

Substituting this form into Eq. (1.2) and ignoring gravity and the magnetic field gives the standard form of the Navier–Stokes equations for a viscous fluid. In plasmas with non-negligible magnetic fields, however, the stress tensor is considerably more complex (e.g., Braginsky, 1965; Hollweg, 1986).

Internal energy conservation:

$$\rho\frac{de}{dt} + p\nabla \cdot \mathbf{v} = \nabla\cdot(\underline{\boldsymbol{\kappa}} \cdot \nabla\mathbf{T}) + (\underline{\boldsymbol{\eta}}_e \cdot \mathbf{j}) \cdot \mathbf{j} + Q_\nu - Q_r, \tag{1.5}$$

where

$$e = \frac{p}{(\gamma - 1)\rho}$$

is the internal energy per unit mass, $\underline{\boldsymbol{\kappa}}$ is the thermal conductivity tensor, T is the temperature, $\underline{\boldsymbol{\eta}}_e$ is the electrical resistivity tensor, Q_ν is the heating by viscous dissipation, Q_r is the radiative energy loss, and γ is the ratio of specific heats. In terms of the stress tensor ($\underline{\mathbf{S}}$), Q_ν is

$$Q_\nu = \mathbf{v} \cdot (\nabla \cdot \underline{\mathbf{S}}) - \nabla \cdot (\underline{\mathbf{S}} \cdot \mathbf{v}). \tag{1.6}$$

In many astrophysical and solar applications, the plasma is optically thin and so the radiative loss term in Eq. (1.5) can be expressed as

$$Q_r = \rho^2\, Q(T),$$

where $Q(T)$ is a function describing the temperature variation of the radiative loss (Fig. 11.9).

Faraday's equation:

$$\nabla \times \mathbf{E} = -\frac{\partial \mathbf{B}}{\partial t}, \tag{1.7}$$

where $\mathbf{E}$ is the electric field.

In MHD the usual displacement term ($\epsilon_0 \, \partial \mathbf{E}/\partial t$, where ϵ_0 is the permittivity of free space) in Maxwell's equations is negligible and so the current is related to the field ($\mathbf{B}$) simply by

Ampère's law:

$$\nabla \times \mathbf{B} = \mu \, \mathbf{j}. \tag{1.8}$$

Because the divergence of the curl is zero, Eq. (1.8) immediately gives us the result that $\nabla \cdot \mathbf{j} = 0$, so that the electric current lines have no monopolar sources: they form closed paths unless they are ergodic or go off to infinity. Also, substitution of Eq. (1.8) for $\mathbf{j}$ in Eq. (1.2) enables the $\mathbf{j} \times \mathbf{B}$ force term to be replaced by $-\nabla[B^2/(2\mu)] + (\mathbf{B} \cdot \nabla)\mathbf{B}/\mu$. This form shows that the magnetic force in Eq. (1.2) can be divided into a magnetic pressure force $-\nabla[B^2/(2\mu)]$ and a magnetic tension force $(\mathbf{B} \cdot \nabla)\mathbf{B}/\mu$.

Gauss's law:

$$\nabla \cdot \mathbf{B} = 0. \tag{1.9}$$

Ohm's law:

$$\mathbf{E}' = \mathbf{E} + \mathbf{v} \times \mathbf{B} = \underline{\boldsymbol{\eta}}_e \cdot \mathbf{j}. \tag{1.10}$$

In many applications it is sufficient to write the electrical resistivity tensor as $\underline{\boldsymbol{\eta}}_e = \eta_e \, \delta_{ij}$, where η_e (the scalar electrical resistivity) is the inverse of the electrical conductivity (σ) so that

$$\mathbf{E}' = \mathbf{E} + \mathbf{v} \times \mathbf{B} = \frac{\mathbf{j}}{\sigma}. \tag{1.10a}$$

Here $\mathbf{E}' = \mathbf{E} + \mathbf{v} \times \mathbf{B}$ gives the Lorentz transformation from the electric field ($\mathbf{E}$) in a laboratory frame of reference to the electric field ($\mathbf{E}'$) in a frame moving with the plasma. It is important to note that Ohm's Law states that it is the electric field ($\mathbf{E}'$) in the moving frame (rather than in the laboratory frame) that is proportional to the current.

Equation of state:

$$p = \mathcal{R} \, \rho \, T \; = \; n \, k_B \, T, \tag{1.11}$$

where $\mathcal{R}$ is the universal gas constant ($8300 \, \mathrm{m^2 \, s^{-2} \, deg^{-1}}$), n is the total number of particles per unit volume, and k_B is Boltzmann's constant. The density can be written in terms of n as

$$\rho = n \, \overline{m},$$

where $\overline{m}$ is the mean particle mass, so that $k_B/\mathcal{R} = \overline{m}$. For a hydrogen plasma with electron number density n_e, the pressure becomes

$$p = 2n_e k_B T$$

and the plasma density may be written

$$\rho \approx n_e m_p,$$

where m_p is the proton mass.

The above system of time-dependent equations constitutes a set of 16 coupled equations for 15 unknowns ($\mathbf{v}, \mathbf{B}, \mathbf{j}, \mathbf{E}$, ρ, p, and T). Thus, it may seem that the system is over-determined. However, Gauss's law, Eq. (1.9), for the divergence of the magnetic field is a relatively weak constraint which has the status only of an initial condition. Taking the divergence of Faraday's equation, Eq. (1.7), and recalling that the divergence of the curl is always zero, we find that $\partial(\nabla \cdot \mathbf{B})/\partial t = 0$, so that, if $\nabla \cdot \mathbf{B}$ is zero initially, it will remain zero for all time. Therefore, given a divergence-free initial state, Gauss's law follows from Faraday's equation. It is interesting to note that the steady-state version of these equations has a different mathematical structure, with $\nabla \cdot \mathbf{B} = 0$ becoming a genuine equation. Instead, Faraday's equation (1.7) essentially represents only two rather than three equations, since the three equations $\nabla \times \mathbf{E} = \mathbf{0}$ may be replaced by the three equations $\mathbf{E} = -\nabla\Phi$ together with the introduction of an extra (sixteenth) variable Φ.

1.2.2 Other Useful Forms

Other useful forms can be obtained by combining the above equations. For example, the variables $\mathbf{E}$, $\mathbf{j}$, and T in the above system can easily be eliminated by substitution. Consequently, the eight remaining unknowns ($\mathbf{B}, \mathbf{v}, p$, and ρ) are usually thought of as the primary variables of MHD. For example, Faraday's equation can be combined with Ampère's law and Ohm's law to obtain the

Induction equation:

$$\frac{\partial \mathbf{B}}{\partial t} = \nabla \times (\mathbf{v} \times \mathbf{B}) - \nabla \times (\eta \nabla \times \mathbf{B}),$$

where $\eta = (\mu\sigma)^{-1} = \eta_e/\mu$ is the magnetic diffusivity. If η is uniform, then

$$\frac{\partial \mathbf{B}}{\partial t} = \nabla \times (\mathbf{v} \times \mathbf{B}) + \eta \nabla^2 \mathbf{B}. \tag{1.12}$$

This is the basic equation for magnetic behaviour in MHD, and it determines **B** once **v** is known. In the electromagnetic theory of fixed conductors, the electric current and electric field are primary variables with the current driven by electric fields. In such a fixed system the magnetic field is a secondary variable derived from the currents. However, in MHD the basic physics is quite different, since the plasma velocity (**v**) and magnetic field (**B**) are the primary variables, determined by the induction equation and the equation of motion, while the resulting current density (**j**) and electric field (**E**) are secondary and may be deduced from Eqs. (1.8) and (1.10a) if required (Parker, 1996).

For a collisional plasma with a strong magnetic field but a relatively weak electric field, the magnetic diffusivity is approximately given by Spitzer's formula (Spitzer, 1962; Schmidt, 1966), namely

$$\eta_\perp = \frac{c^2 e^2 m_e^{1/2}}{3(2\pi)^{3/2}\epsilon_0} \ln\Lambda\,(k_B T_e)^{-3/2} = 1.05\times 10^8\, T_e^{-3/2}\,\ln\Lambda\,\mathrm{m^2\,s^{-1}}, \quad (1.13)$$

where m_e is the electron mass, T_e the electron temperature, and $\ln\Lambda$ is the coulomb logarithm (Holt and Haskell, 1965), given approximately by

$$\ln\Lambda = \begin{cases} 16.3 + \frac{3}{2}\ln T - \frac{1}{2}\ln n, & T < 4.2\times 10^5\,\mathrm{K}, \\ 22.8 + \ln T - \frac{1}{2}\ln n, & T > 4.2\times 10^5\,\mathrm{K}. \end{cases} \quad (1.14)$$

For the final expression in Eq. (1.13) we have assumed a hydrogen plasma. The $\perp$ subscript indicates that Eq. (1.13) is the resistivity in a direction perpendicular to the magnetic field. If the current flows along the field, or if the plasma is unmagnetized, the parallel magnetic diffusivity is $\eta_\parallel \approx \eta_\perp/2$.

Since the collisional theory used to calculate Eq. (1.13) is a first-order expansion in powers of $1/\ln\Lambda$, the theory is only accurate when $\ln\Lambda \gg 1$. In laboratory plasmas, $\ln\Lambda$ is typically about 10, in the solar corona it is about 20, and in the magnetosphere it is about 30. Thus, transport coefficients such as Eq. (1.13) are only accurate to a few percent. The requirement that the electric field be weak means that the electric field must be less than the Dreicer field (E_D) for runaway electrons [see Eq. (1.66)], while the condition that the magnetic field be strong means that the electron gyro-radius must be much smaller than the mean-free path (λ_{mfp}) for electron-ion collisions.

If V_0, L_0 are typical velocity and length-scales, the ratio of the first to the second term on the right-hand side of Eq. (1.12) is, in order of magnitude, the magnetic Reynolds number

$$R_m = \frac{L_0 V_0}{\eta}.$$

Thus, for example, in the solar corona above an active region, where $T \approx 10^6$ K, $\eta \approx 1\,\mathrm{m^2\,s^{-1}}, L_0 \approx 10^5\,\mathrm{m}, V_0 \approx 10^4\,\mathrm{m\,s^{-1}}$, we find $R_m \approx 10^9$, and so the second term on the right of Eq. (1.12) is completely negligible. In turn, Eq. (1.10a) reduces to $\mathbf{E} = -\mathbf{v} \times \mathbf{B}$ to a very high degree of approximation. This is the case in almost all of the solar atmosphere, indeed in almost all of the plasma universe. The only exception is in regions (such as current sheets) where the length-scale is extremely small – so small that $R_m \lesssim 1$ and the second terms on the right-hand sides of Eqs. (1.10a) and (1.12) become important.

If $R_m \ll 1$, the induction equation reduces to

$$\frac{\partial \mathbf{B}}{\partial t} = \eta \nabla^2 \mathbf{B}, \tag{1.15}$$

and so $\mathbf{B}$ is governed by a diffusion equation, which implies that field variations (irregularities) on a scale L_0 diffuse away on a time-scale of

$$\tau_d = \frac{L_0^2}{\eta}, \tag{1.16}$$

which is obtained simply by equating the orders of magnitude of both sides of Eq. (1.15). The corresponding magnetic diffusion speed at which they slip through the plasma is

$$v_d = \frac{L_0}{\tau_d} = \frac{\eta}{L_0}. \tag{1.17}$$

With $\eta \approx 1\,\mathrm{m^2\,s^{-1}}$ and $L_0 = 10^8$ m, the decay-time for a sunspot is 30,000 yr, so that the process whereby sunspots disappear in a few weeks cannot just be diffusion. Note that the corresponding viscous diffusion speed, which arises from the equation of motion when viscous forces are included, is $v_D = \nu/L_0$.

The main reason for variations in R_m from one phenomenon to another is variations in the appropriate length-scale (L_0). If $R_m \gg 1$, the induction equation becomes

$$\frac{\partial \mathbf{B}}{\partial t} = \nabla \times (\mathbf{v} \times \mathbf{B}).$$

Although the electric field and current density are usually ignored during the process of solving the MHD equations, valuable insight can often be gained by determining the electric field and current density afterwards. In this regard, it is often helpful to introduce the concepts of the electric scalar potential (Φ) and magnetic vector potential ($\mathbf{A}$). Defining $\mathbf{A}$ from $\mathbf{B} = \nabla \times \mathbf{A}$ (to within a gauge), one then writes Faraday's equation and Ampère's